WIDEBAND WAVEFORM DESIGN FOR ROBUST TARGET DETECTION

Ashkan Panahi, Marie Ström, Mats Viberg

Signal Processing Group, Signals and Systems Department, Chalmers University, Gothenburg, Sweden

ABSTRACT

Future radar systems are expected to use waveforms of a high bandwidth, with an advantage of an improved range resolution. Herein, a technique to design robust wideband waveforms is developed. The context is detection of a single object with partially unknown parameters. The technique achieves an optimal detection speed for a desired resolution, maintaining a high detection performance. Many radar systems also require fast adaptation to a variable environment. Hence, the technique is devoted to rapidly design waveforms. In terms of probabilities of detection and false alarm, numerical evaluation shows the efficiency of the method when compared with a chirp signal and a Gaussian pulse.

***Index Terms*—** robust detection, detection speed, waveform design

1. INTRODUCTION

Signal processing techniques for radar systems have to a great extent focused on narrowband signals. At this time, signal generators are able to synthesize arbitrary signals with a large bandwidth [1, 2]. This provides interesting new opportunities, e.g., achieving an increased range resolution compared to a narrowband counterpart [3–6]. However, the simplifying narrowband assumption, where velocity is approximated as a frequency shift, is not valid [6]. This substantially complicates the pulse and receiver filter design, as estimation of time-delay and Doppler-shift cannot be separated in time and frequency. One practical solution is to scan the delay-Doppler parameter space by multiple transmissions and utilize simple matched filter receivers to perform detection over a small region of the parameter space through each pulse transmission. In this case, a high quality of detection simply depends on a high filter output from the interior of the region and a low output by the exterior.

This approach relates to other contributions in the area. For example, design of wideband ambiguity functions with narrow peaks for Orthogonal-Frequency-Division-Multiplexing signals is considered in [7, 8]. In [9] various techniques for designing narrowband or wideband waveforms are discussed. Interesting analysis of wideband radar systems from various perspectives are also found in [10–12]. It is observed that the above techniques provide high detection performance with small detection regions, which insures a high resolution. However, decreasing the detection region size leads to an increase in the number of transmissions, subsequently resulting in an increased overall scan time. Unfortunately, the previous studies do not discuss a method to control the region size.

To combat this issue, this work proposes a method to design waveforms that robustly detect targets in specified regions of the parameter space leading to a desired scan time. Although this leads to detections of a restricted resolution, it is easy to adapt a secondary super-resolution detection procedure [13–15] based on the original estimates. This provides a highly flexible design with low complexity.

The design is formulated as an optimization by means of a Gaussian basis expansion, and the performance is, i.a., presented in terms of probabilities of detection and false alarm. A fast solution of the optimization is proposed. This is useful when a rapid online modification of the detection scheme is necessary. The performance is evaluated by means of numerical experiments.

2. ELEMENTS OF THE PROBLEM

Consider a stationary bistatic radar system that, on the transmitter side, employs M waveform generators each connected to an antenna element. The receiver side comprises one antenna element connected to a filter bank. Each generator samples a signal composed of N basis functions $\psi_{m,n}(t)$, where m and n are the antenna and basis label, respectively, i.e.,

$$\tilde{x}_m(t) = \sum_{n=1}^{N} s_{m,n}\psi_{m,n}(t). \tag{1}$$

where $\tilde{x}_m$ is a baseband waveform at the mth signal generator, and $s_{m,n}$ is a complex scalar coefficient. The received signal is a mixture of the reflected transmitted waveforms, and can be expressed, for a point target, as

$$y(t;\tau,\mu) = \sigma_t \sum_{m=1}^{M} x_m(\mu(t-\tau-\tau_m(\phi))) + n(t). \tag{2}$$

where σ_t is an object's reflection coefficient, τ denotes a time-delay from the zero-phase sensor to a receiver, μ is a time-scaling related to a velocity of an object [5, 6], and $\tau_m(\phi)$ is given by an inter-element spacing and a spatial direction, ϕ, towards a object. This direction, azimuth and/or elevation, is assumed to be known. If this is not the case, a beamforming technique, see, e.g., [16–18], is necessary. In (2), $x_m(t) =$

$\tilde{x}_m(t)e^{j\omega_c t}$ is centered around the system's carrier frequency $f_c = \omega_c/2\pi$ and $n(t)$ is a white Gaussian noise.

At the receiver side the down-converted signal, $\tilde{y}(t;\tau,\mu) = y(t;\tau,\mu)e^{-j\omega_c t}$, is passed through a filter bank, i.e.,

$$r(\tau,\tau',\mu,\mu') = \int h^*(t;\tau',\mu')\tilde{y}(t;\tau,\mu)dt. \tag{3}$$

Here, $(\cdot)^*$ denotes the complex conjugate. If a so-called matched filter structure [19, 20] is employed, the correlating filters, $h(t;\tau',\mu')$, are equal to the received signal calculated from their corresponding transmission model.

Assume that the basis kernels, $\psi_{m,n}(t)$, are Gaussian. This particular choice of functions results in that (3), omitting noise contributions, can be analytically calculated to

$$r(\tau_0,\mu,\mu') = \sum_{\substack{m,m'\in\mathcal{M}\\ n,n'\in\mathcal{N}}} \frac{\sigma_t\sqrt{\mu\mu'}s_{m,n}s_{m',n'}e^{-j\omega_c\mu'(\tau_0+\tau_{m,m'})}}{\sqrt{2\pi(\mu^2\sigma^2_{m',n'}+\mu'^2\sigma^2_{m,n})}} \cdot e^{-\frac{(\mu'\mu_{m,n}-\mu\mu_{m',n'}+\mu\mu'(\tau_0+\tau_{m,m'}))^2}{2(\mu^2\sigma^2_{m',n'}+\mu'^2\sigma^2_{m,n})}} e^{\omega_c(\mu-\mu')(j\mu_G-\frac{\omega_c}{2}(\mu-\mu')\sigma^2_G)}, \tag{4}$$

where $\mathcal{M} = \{1\ldots M\}$, $\mathcal{N} = \{1\ldots N\}$, $\sigma^2_{m,n}$ and $\mu_{m,n}$ correspond to the variance and the mean of the nth basis kernel sampled by the mth signal generator, respectively, $\tau_0 = \tau - \tau'$, $\tau_{m,m'} = \tau_m(\phi) - \tau_{m'}(\phi)$, and

$$\mu_G = \frac{\mu\mu_{m,n}\sigma^2_{m',n'} + \mu'(\mu_{m',n'} - \mu'(\tau_0+\tau_{m,m'}))\sigma^2_{m,n}}{\mu^2\sigma^2_{m',n'}+\mu'^2\sigma^2_{m,n}}$$

$$\sigma^2_G = \frac{\sigma^2_{m,n}\sigma^2_{m',n'}}{\mu^2\sigma^2_{m',n'}+\mu'^2\sigma^2_{m,n}}.$$

The expression in (4) is equivalently written in a matrix form as $r(\tau_0,\mu,\mu') = \sigma_t\mathbf{s}^H\mathbf{R}(\tau_0,\mu,\mu')\mathbf{s}$, where $\mathbf{s} = [s_{1,1}\ldots s_{N,1}, s_{1,2}\ldots s_{N,2}\ldots s_{N,M}]^T$ and $\mathbf{R}(\tau_0,\mu,\mu')$ contains the entries

$$R_{m,m',n,n'}(\tau_0,\mu,\mu') = \frac{\sigma_t\sqrt{\mu\mu'}e^{-j\omega_c\mu'(\tau_0+\tau_{m,m'})}}{\sqrt{2\pi(\mu^2\sigma^2_{m',n'}+\mu'^2\sigma^2_{m,n})}} \cdot e^{-\frac{(\mu'\mu_{m,n}-\mu\mu_{m',n'}+\mu\mu'(\tau_0+\tau_{m,m'}))^2}{2(\mu^2\sigma^2_{m',n'}+\mu'^2\sigma^2_{m,n})}} e^{\omega_c(\mu-\mu')(j\mu_G-\frac{\omega_c}{2}(\mu-\mu')\sigma^2_T)}, \tag{5}$$

in a proper order.

2.1. Robust Waveform Design Based on Statistical Performance

Target detection is formulated as a statistical problem as follows. Take a region $\mathcal{S}$ of the parameter pairs (μ,τ) in which a good detection performance is desired. The detection is based on the output r from a filter matched to a nominal point $(\tau',\mu') \in \mathcal{S}$.

The idea is to develop a simple decision rule for r, which identifies whether a target is present in $\mathcal{S}$ or not. The problem can be formulated as a composite hypothesis testing, where $\mathcal{H}_0$ denotes the hypothesis that no source is present, in which r is generated by a white Gaussian noise processes, and $\mathcal{H}_1$ denotes the composite hypothesis of source existence. Then, the likelihood functions under the different hypotheses are

$$\begin{aligned} &\mathcal{H}_0:\ r \sim \mathcal{N}(0, \sigma^2\mathbf{s}^H\mathbf{R}_0\mathbf{s}) \\ &\mathcal{H}_1:\ r\ \sim \mathcal{N}(\sigma_t\mathbf{s}^H\mathbf{R}(\tau_0,\mu,\mu')\mathbf{s}, \sigma^2\mathbf{s}^H\mathbf{R}_0\mathbf{s}), \end{aligned} \tag{6}$$

where $\mathbf{R}_0 = \mathbf{R}(\tau_0 = 0,\mu',\mu')$ and σ^2 denotes the noise power. The pair (τ_0,μ) denotes the unknown true parameters. Later, we simply refer to it as θ. Let us consider the Generalized Likelihood Ratio Test (GLRT) [21], which can be written as

$$\min_{\theta,\sigma_t} |r - \sigma_t\mathbf{s}^H\mathbf{R}(\theta)\mathbf{s}|^2 + \gamma \gtrless |r|^2, \tag{7}$$

where the argument μ' is dropped as its value is assumed to be fixed, and γ is a threshold. As σ_t is free the GLRT simplifies to

$$\gamma \gtrless |r|, \tag{8}$$

which is a simple power thresholding scheme.

For this detector probabilities of detection, P_D, and false alarm, P_{FA}, can be calculated to

$$\begin{aligned} P_D(\theta,\sigma_t,\gamma) &= \frac{1}{\pi\mathbf{s}^H\mathbf{R}_0\mathbf{s}\sigma^2}\int_{|r|>\gamma} e^{-\frac{|r-\sigma_t\mathbf{s}^H\mathbf{R}(\theta)\mathbf{s}|^2}{\mathbf{s}^H\mathbf{R}_0\mathbf{s}\sigma^2}}\mathrm{d}\nu(r) \\ P_{FA} &= \frac{1}{\pi\mathbf{s}^H\mathbf{R}_0\mathbf{s}\sigma^2}\int_{|r|>\gamma} e^{-\frac{|r|^2}{\mathbf{s}^H\mathbf{R}_0\mathbf{s}\sigma^2}}\mathrm{d}\nu(r), \end{aligned} \tag{9}$$

where $\nu(.)$ denotes the Lebesgue measure on the complex plane of r.

To optimize waveforms, consider the worst detection performance $P_D(\theta,\sigma_t,\gamma)$ over all scenarios defined by (θ,σ_t), where $P_{FA} = \alpha$ is fixed. One may define the best design as the one maximizing the worst detection. Unfortunately, direct calculation shows that this approach fails in the current occasion as the worst detection performance is independent of the choice of waveform. However, this can be easily corrected by a minor modification of the definition of optimality, which is given in *Definition 1*, where $P_{D,\text{worst}}$, the worst detection performance.

Definition 1 *A design* $\mathbf{s}$ *is optimal for a given value of* α *if for sufficiently small values of* ϵ*, the set* $\mathcal{S}_\epsilon$ *of* $\epsilon-$*worse scenarios, defined by*

$$\mathcal{S}_\epsilon = \{(\theta,\sigma_t) \mid |P_D(\theta,\sigma_t) < P_{D,\textit{worst}} + \epsilon\} \tag{10}$$

has a minimal area (Lebesgue measure) in any compact region.

This gives a design, where it is least likely to encounter a low performance. The following theorem provides a practical method to realize this design.

Theorem 1 *The optimal design in the sense of Definition 1 is a solution to the following optimization*

$$\begin{aligned} \max_{\mathbf{s}} \min_{\theta} \quad & |\mathbf{s}^H \mathbf{R}(\theta)\mathbf{s}| \\ \textit{s.t.} \quad & \mathbf{s}^H \mathbf{R}_0 \mathbf{s} = 1. \end{aligned} \tag{11}$$

The reader may notice that (11) could be directly introduced and intuitively validated. It is simple to verify that $|\mathbf{s}^H \mathbf{R}(\theta)\mathbf{s}|$ and $\mathbf{s}^H \mathbf{R}_0 \mathbf{s}$ are the share of signal and noise in the filter output energy over $\mathcal{S}$, respectively. Thus, (11) promotes a uniformly high signal-output energy. However, the above calculations tie (11) to a statistically sound detection approach.

Clearly, (11) guarantees high detection rate, but it does not consider false detection due to coupling between the filter and out-of-box sources. However, it is expected that the finite energy constraint automatically enforces low sidelobe energy.

3. PROPOSED METHOD FOR SOLVING (11)

It is difficult to exactly solve (11), as $\mathbf{R}(\theta)$ is in general not Hermitian. One approximate solution is to consider the inner optimization over a finite number of grid points, $\theta_1, \theta_2, \ldots, \theta_l$. Then, (11) can be written as

$$\begin{aligned} \max_{\mathbf{s}} \min_{\lambda_1,\lambda_2,\ldots,\lambda_l} \quad & \sum_k |\mathbf{s}^H \mathbf{R}(\theta_k)\mathbf{s}|\lambda_k \\ \text{s.t.} \quad & \mathbf{s}^H \mathbf{R}_0 \mathbf{s} = 1, \quad \sum_k \lambda_k = 1, \end{aligned} \tag{12}$$

where λ_k is a positive number. By changing the order of minimization and maximization in (12) we obtain the following suboptimal design, which is simpler to solve [22].

$$\begin{aligned} \min_{\lambda_1,\lambda_2,\ldots,\lambda_l} \max_{\mathbf{s}} \quad & \sum_k |\mathbf{s}^H \mathbf{R}(\theta_k)\mathbf{s}|\lambda_k \\ \text{s.t.} \quad & \mathbf{s}^H \mathbf{R}_0 \mathbf{s} = 1, \quad \sum_k \lambda_k = 1. \end{aligned} \tag{13}$$

As opposed to the uniformly optimal design in the original order, the change of order results in an optimization considering average performance weighted by $\{\lambda_k\}$. Now, the inner optimization in (13) is simplified as follows. Consider the eigenvalue decomposition of $\mathbf{R}_0$, i.e., $\mathbf{R}_0 = \mathbf{U}\Sigma\mathbf{U}^H = \mathbf{U}_0\Sigma_0\mathbf{U}_0^H$, where Σ_0 and $\mathbf{U}_0$ are the nonzero blocks of Σ and its corresponding columns of $\mathbf{U}$, respectively. Let $\mathbf{u} = \mathbf{\Sigma_0}^{\frac{1}{2}}\mathbf{U_0}^H\mathbf{s}$, which implies that any vector $\mathbf{s}$ is uniquely decomposed in terms of its corresponding $\mathbf{u}$ as

$$\mathbf{s} = \mathbf{U_0}\mathbf{\Sigma_0}^{-\frac{1}{2}}\mathbf{u} + \mathbf{U_1}\mathbf{p}, \tag{14}$$

where $\mathbf{p}$ is a suitable vector and $\mathbf{U_1}$ spans the null space of R_0. Note that, any vector $\mathbf{s}$ with $\mathbf{s}^H \mathbf{R}_0 \mathbf{s} = 0$ corresponds to zero-energy, which leads to a zero output-signal. This clearly means that $\mathbf{R}(\theta)\mathbf{U}_1 = 0$ for every θ. Thus, the term U_1 does not have any effect on the waveform design, and the inner optimization in (13) can be expressed as

$$\begin{aligned} \max_{\mathbf{u}} \quad & \sum_k \lambda_k |\mathbf{u}^H \tilde{\mathbf{R}}(\theta_k)\mathbf{u})| \\ \text{s.t.} \quad & \|\mathbf{u}\|_2^2 = 1, \end{aligned} \tag{15}$$

where $\tilde{\mathbf{R}}(\theta_k) = \mathbf{\Sigma}_0^{-1/2}\mathbf{U_0}^H\mathbf{R}(\theta_k)\mathbf{U_0}\mathbf{\Sigma_0}^{-\frac{1}{2}}$.

To solve (15), we propose the following efficient scheme. First, note that, $|\alpha| = \max_{\phi} \Re(e^{-j\phi}\alpha)$. Thus, (15) is equivalently written as

$$\begin{aligned} & \max_{\mathbf{u},\phi_1,\phi_2,\ldots,\phi_l} \sum_k \lambda_k \Re(e^{-j\phi_k}\mathbf{u}^H \tilde{\mathbf{R}}(\theta_k)\mathbf{u}) \\ & = \max_{\mathbf{u},\phi_1,\phi_2,\ldots,\phi_l} \mathbf{u}^H \mathbf{M}(\phi_1,\phi_2,\ldots,\phi_l)\mathbf{u}, \end{aligned} \tag{16}$$

where

$$\mathbf{M}(\phi_1,\phi_2,\ldots,\phi_l) = \sum_k \lambda_k (e^{-j\phi_k}\tilde{\mathbf{R}}(\theta_k) + e^{j\phi_k}\tilde{\mathbf{R}}^H(\theta_k)). \tag{17}$$

As the optimization is performed over all unit vectors $\mathbf{u}$, the solution for a fixed choice of $\phi_1, \ldots, \phi_l$ is the eigenvector of $\mathbf{M}$ corresponding to the largest eigenvalue, which we denote by $\mathbf{u}_m(\mathbf{M})$ and $\lambda_m(\mathbf{M})$, respectively. Accordingly, we propose the following cyclic solution of the inner optimization.

1. Start from an arbitrary choice of ϕ_k^0 and set $r = 1$.
2. Get $\mathbf{M}^{r-1} = \mathbf{M}(\phi_1^{r-1}, \ldots, \phi_n^{r-1})$ and set $\mathbf{u}^r = \mathbf{u}_m(\mathbf{M}^{r-1})$ by calculating $\lambda_m(\mathbf{M}(\phi^{r-1}))$.
3. Evaluate ϕ_k^n as the argument of the complex number $(\mathbf{u}^r)^H\tilde{\mathbf{R}}(\theta_k)\mathbf{u}^r$, update r to $r+1$ and go to step 2.

Step 2 and step 3 increase the cost of (16) with respect to $\mathbf{u}$ and ϕ. Thus, the cost monotonically increases, which guarantees convergence.

Once a solution, say $\bar{\mathbf{u}}$, for the inner optimization and given values of λ_k is obtained, a local optimization technique such as steepest descent is performed to update λ_k for the outer minimization. Although, the gradient, ∇F, of the cost $F = F(\lambda_1, \ldots, \lambda_l)$ at a given point is simple to compute, applying a steepest decent technique is generally difficult. However, the number of grid points, l, in (12) may be significantly low as a result of sufficient correlation between conceivable return signals. In fact, we employ only a pair of properly selected grid points, typically the corner points of a parameter box, from which the outer optimization can be substantially simplified to

$$\min_{0\leq\lambda\leq 1} F(\lambda, 1-\lambda), \tag{18}$$

and a resulting 1-dimensional optimization is either carried out by a grid search or a bisection method [23].

4. NUMERICAL VALIDATION

For different choices of regions in which a robust performance is desired, the efficiency of the proposed algorithm is presented in terms of average and minimum correlation as well as Receiver Operating Characteristic (ROC) [24] curves. The number of waveform generators is $M = 3$ for which $N = 30$ basis functions are generated. The system has a bandwidth-time product of 200, the nominal value μ' is 0.94, and the target's reflection coefficient is set to $\sigma_t = 1$.

The Gaussian basis are generated with mean values, μ_k, uniformly located over the pulse duration, and standard deviations selected randomly within an interval $[\sigma_{\min,k}\ \sigma_{\max,k}]$, where $\sigma_{\max,k}$ is such that the effective interval between $\mu_k \pm 3\sigma_k$ is ensured to lie within the pulse time, and $\sigma_{\min,k}$ restricts the highest effective frequency component. Results are averaged over 100 independent draws of standard deviations.

The region in which the performance is evaluated is chosen as a box, which varies in size. The smallest box is within the confines of $\mu \in [\mu_0 - \epsilon_\mu, \mu_0 + \epsilon_\mu]$ and $\tau \in [-\epsilon_\tau, \epsilon_\tau]$, where ϵ_μ and ϵ_τ are determined with respect to twice the system's resolution limits. In order to investigate the effect of varying uncertainty, the box size increases with a factor β to ϵ_μ/β and ϵ_τ/β, where $\beta = [1, \ldots, 0.1]$. A scan time can be defined as the number of necessary regions multiplied with the pulse time and spatial sectors, neglecting processing time. Then, the constant β^2 relates to a relative scan time, as it is proportional to the number of necessary regions, i.e., a smaller β divides the search space into fewer regions.

The minimum and average in-box correlation, $|\mathbf{s}^H\mathbf{R}(\theta)\mathbf{s}|$, are presented in Table 1 and Table 2. The correlation properties are evaluated over a dense grid and then taking average or minimum, respectively. The outcome is compared with the cases where a chirp pulse and a single Gaussian pulse is transmitted from each signal generator, with the same bandwidth-time product. It should be noted that the chirp pulse provides a high resolution, and is not expected to give a robust performance. Figure 1 shows the ROC curves, which are calculated through a Monte Carlo simulation using the estimator in (8) with 10^6 noise realizations, and a Signal-to-Noise Ratio (SNR) of 10 dB. The Figure shows the characteristics for a varying threshold γ, and also compared with a case where coefficients are randomly selected. Curves corresponding to $\beta^2 = 1$ illustrates performance in which the smallest box is selected. The performance decreases when expanding the region. However, it exhibits a robust behavior for relatively large boxes.

Table 1: Average correlation properties.

Algorithm	$\beta^2 = 1$	$\beta^2 = 0.36$	$\beta^2 = 0.16$	$\beta^2 = 0.04$
Proposed alg.	0.99	0.97	0.94	0.65
Gaussian	0.97	0.88	0.80	0.60
Chirp	0.30	0.21	0.15	0.09

Table 2: Minimum correlation properties.

Algorithm	$\beta^2 = 1$	$\beta^2 = 0.36$	$\beta^2 = 0.16$	$\beta^2 = 0.04$
Proposed alg.	0.98	0.93	0.85	0.41
Gaussian	0.88	0.70	0.42	0.1
Chirp	0.0039	0.0018	0.0018	0.0016

The last part presents how an out-of-region source affects the ROC curve. This source increases probability of false alarm if its return is highly correlated with the matched filter for the region of interest. The position of the source is randomly generated outside the interval of μ and τ. Results shown in Figure 2 illustrates ROC curves when the out-of-region source has a reflection coefficient of $\sigma_{os} = 1$, the outcome when $\sigma_{os} = -1$ coincides with $\sigma_{os} = 1$.

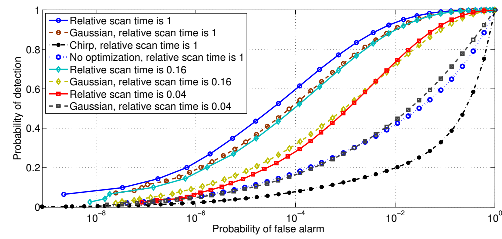

Fig. 1: ROC curves when the SNR is 10 dB for regions specified by $\beta^2 = [1, 0.16, 0.04]$.

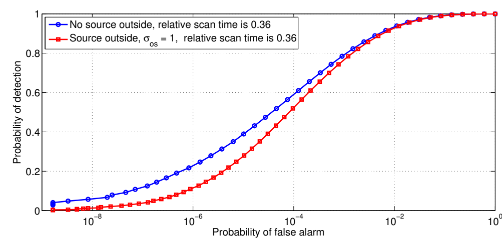

Fig. 2: ROC curve when an out-of-region source with $\sigma_{os} = 1$ is present. The SNR is 10 dB and $\beta^2 = 0.36$.

5. CONCLUSIONS

For a wideband radar, we considered a robust technique for waveform design within relatively wide parameter ranges, which ensures a desirable detection time. The method was developed from a statistical framework for detecting a single target, and simplified by approximation to obtain a tractable design. Being robust implies that the waveforms are not designed to provide good resolution properties. Therefore, a next step is to apply a super-resolution technique to the restricted area obtained from this first stage.

The correlating filters at the receiver side were selected to have a matched filter structure. We remark that, a different kind of filter design, e.g., [25–27] might result in better performance, which is a topic for future investigation.

The method ensured reliable detection in the desired range of target parameters. The probabilities of detection and false alarm are illustrated with ROC curves, which showed a small loss of performance when increasing the desired region of reliable detection up to a certain size. The outcome was compared with two transmit signal schemes and showed an increased performance for the investigated problem. Note that, chirp signals have good resolution properties, which makes them unsuitable for the discussed application. It was also seen that in presence of an out-of-region source the detection properties are only slightly affected, which implied that the design promoted a low sidelobe energy.

6. REFERENCES

[1] J. Han and C. Nguyen, "A new ultra-wideband, ultra-short monocycle pulse generator with reduced ringing," *Microwave and Wireless Components Letters, IEEE*, vol. 12, no. 6, pp. 206–208, June 2002.

[2] Y. Zhu, J. Zuegel, J. Marciante, and H. Wu, "Distributed waveform generator: A new circuit technique for ultra-wideband pulse generation, shaping and modulation," *Solid-State Circuits, IEEE Journal of*, vol. 44, no. 3, pp. 808–823, March 2009.

[3] J. D. Taylor, *Introduction to ultra-wideband radar systems*. CRC press, 1994.

[4] H. Khan, W. Malik, D. Edwards, and C. Stevens, "Ultra wideband multiple-input multiple-output radar," in *Radar Conference, 2005 IEEE International*, May 2005, pp. 900–904.

[5] M. Hussain, "Ultra-wideband impulse radar- an overview of the principles," *Aerospace and Electronic Systems Magazine, IEEE*, vol. 13, no. 9, pp. 9–14, 1998.

[6] L. Weiss, "Wavelets and wideband correlation processing," *Signal Processing Magazine, IEEE*, vol. 11, no. 1, pp. 13–32, 1994.

[7] S. Sen and A. Nehorai, "Adaptive design of ofdm radar signal with improved wideband ambiguity function," *Signal Processing, IEEE Transactions on*, vol. 58, no. 2, pp. 928–933, 2010.

[8] ——, "Target detection in clutter using adaptive ofdm radar," *Signal Processing Letters, IEEE*, vol. 16, no. 7, pp. 592–595, July 2009.

[9] H. He, J. Li, and P. Stoica, *Waveform design for active sensing systems: a computational approach*. Cambridge University Press, 2012.

[10] D. Lush and D. Hudson, "Ambiguity function analysis of wideband radars," in *Radar Conference, 1991., Proceedings of the 1991 IEEE National*, 1991, pp. 16–20.

[11] B. Yazici and G. Xie, "Wideband extended range-doppler imaging and waveform design in the presence of clutter and noise," *Information Theory, IEEE Transactions on*, vol. 52, no. 10, pp. 4563–4580, 2006.

[12] G. S. Antonio and D. Fuhrmann, "Beampattern synthesis for wideband mimo radar systems," in *1st IEEE Int. workshop on Comp. Advances in Multi-Sensor Adaptive process.*, Puerto Vallarta, Mexico, December 2005, pp. 105–108.

[13] S. Borison, S. B. Bowling, and K. M. Cuomo, "Super-resolution methods for wideband radar," 1992.

[14] K. M. Cuomo, J. E. Pion, and J. T. Mayhan, "Ultrawide-band coherent processing," *Antennas and Propagation, IEEE Transactions on*, vol. 47, no. 6, pp. 1094–1107, 1999.

[15] J. Moore and H. Ling, "Super-resolved time-frequency analysis of wideband backscattered data," *Antennas and Propagation, IEEE Transactions on*, vol. 43, no. 6, pp. 623–626, 1995.

[16] A. Gershman, "Robust adaptive beamforming in sensor arrays," *AEU International Journal of Electronics and Communications*, vol. 53, no. 6, pp. 305–314, 1999.

[17] J. Li and P. Stoica, *Robust adaptive beamforming*. Wiley Online Library, 2006.

[18] S. A. Vorobyov, A. B. Gershman, and Z.-Q. Luo, "Robust adaptive beamforming using worst-case performance optimization: A solution to the signal mismatch problem," *Signal Processing, IEEE Transactions on*, vol. 51, no. 2, pp. 313–324, 2003.

[19] M. Skolnik, *Radar Handbook*. New York, NY: The McGraw-Hill Companies, 1976.

[20] ——, *Introduction to Radar Systems*. New York, NY: The McGraw-Hill Companies, 1981.

[21] S. M. Kay, "Fundamentals of statistical signal processing: Detection theory, vol. 2," 1998.

[22] M. S. Bazaraa, H. D. Sherali, and C. M. Shetty, *Nonlinear programming: theory and algorithms*. John Wiley & Sons, 2013.

[23] R. Fletcher, *Practical methods of optimization*. John Wiley & Sons, 2013.

[24] M. A. Richards, *Fundamentals of radar signal processing*. Tata McGraw-Hill Education, 2005.

[25] M. H. Ackroyd and F. Ghani, "Optimum mismatched filters for sidelobe suppression," *Aerospace and Electronic Systems, IEEE Transactions on*, vol. AES-9, no. 2, pp. 214–218, March 1973.

[26] P. Stoica, J. Li, and M. Xue, "On binary probing signals and instrumental variables receivers for radar," *Information Theory, IEEE Transactions on*, vol. 54, no. 8, pp. 3820–3825, Aug 2008.

[27] ——, "Transmit codes and receive filters for radar," *Signal Processing Magazine, IEEE*, vol. 25, no. 6, pp. 94–109, November 2008.